Article:

Alsaif, A. orcid.org/0000-0002-3057-0720, Bernal, S.A. orcid.org/0000-0002-9647-3106, Guadagnini, M. orcid.org/0000-0003-2551-2187 et al. (1 more author) (2018) Durability of steel fibre reinforced rubberised concrete exposed to chlorides. Construction and Building Materials, 188. pp. 130-142. ISSN 0950-0618

https://doi.org/10.1016/j.conbuildmat.2018.08.122

Durability of Steel Fibre Reinforced Rubberised Concrete Exposed to Chlorides

Abdulaziz Alsaif[a*]**, Susan A. Bernal**[b,c]**, Maurizio Guadagnini**[a]
Kypros Pilakoutas[a]

[a]Department of Civil and Structural Engineering, The University of Sheffield, Sir Frederick Mappin Building, Mappin Street, Sheffield, S1 3JD, UK.

[b]Department of Materials Science and Engineering, The University of Sheffield, Sir Robert Hadfield Building, Mappin Street, Sheffield, S1 3JD, UK

[c] School of Civil Engineering, University of Leeds, Woodhouse Lane, Leeds, LS2 9JT, UK

[*] Corresponding author: email: asaalsaif1@sheffield.ac.uk; Tel: +44 (0) 114 222 5729,
Fax: +44 (0) 114 2225700

Abstract

This study assesses the durability and transport properties of low water/binder ratio (0.35) steel fibre reinforced rubberised concrete (SFRRuC) mixes, which are proposed to be used as flexible concrete pavements. Waste tyre rubber is incorporated in concrete as fine and coarse aggregate replacement and blends of manufactured steel fibres and recycled tyre steel fibres are used as internal reinforcement. The fresh, mechanical and transport properties of plain concrete are compared with those of SFRRuC mixes having different substitutions of rubber aggregates (0, 30 and 60% by volume). The chloride corrosion effects due to exposure to a simulated accelerated marine environment (intermittent wet-dry cycles in 3% NaCl solution) is also evaluated. The results show that, although water permeability (e.g. volume of permeable voids and sorptivity) and chloride ingress increase with rubber content, this increase is minor and water and chlorides permeability are generally within the range of highly durable concrete mixes. No visual signs of deterioration or cracking (except superficial rust) were observed on the surface of the concrete specimens subjected to 150 or 300 days of accelerated chloride corrosion exposure and a slight increase in the mechanical properties is observed. This study shows that the examined low water/binder SFRRuC mixes promote good durability characteristics, making these composite materials suitable for flexible concrete pavement applications.

Keywords: *Rubberised concrete; Steel fibre reinforced concrete; Flexible concrete pavement; Hybrid reinforcement.*

1 Introduction

Several factors are considered when designing road pavements including traffic loading, sub-grade status, environmental conditions, as well as cost and availability of construction materials. Two different systems of pavements are conventionally used in roads construction: flexible asphalt or rigid concrete. A flexible pavement typically consists of a series of layers and its design is based on distributing the load through the component layers. On the other hand, a rigid pavement typically consists of one Portland cement concrete structural layer and its design is based on the flexural resistance of this layer. Flexible asphalt pavements have low stiffness and as such they can better accommodate deformations arising from temperature changes, loads and soil movements, however, lack the durability resistance of rigid concrete pavements which are longer lasting [1]. It is therefore desirable to develop a pavement system with comparable flexibility to asphalt pavement, and ability to withstand higher stresses as well as environmental attack during its service life. One attractive alternative proposed by the authors is concrete pavements that include high amounts of recycled rubber particles (chips and/or crumbs), as a partial replacement of natural aggregates, and recycled steel fibre reinforcement. These composite concretes, referred to as steel fibre reinforced rubberised concretes (SFRRuC), can be designed to have high flexibility similar to asphalt and flexural strengths similar to steel fibre reinforced concrete (SFRC) [1].

Over the past two decades, research interest in the potential use of waste tyre rubber (WTR) as partial replacement of natural aggregates in the production of concretes (rubberised concretes – RuC) has steadily grown [2-6]. RuC present reduced workability and increased air content, compared to conventional concretes, as a result of the rough surface texture of the rubber particles [4, 7-9]. Though RuC can show higher ductility and increased toughness compared to conventional concrete [8-10], this is at the expense of loss in strength and stiffness [11, 12]. Different strategies to improve the mechanical performance of RuC have been investigated in recent years, including the addition of supplementary cementitious materials to the binder mix to reduce the porosity and aid early age strength development. For example, Raffoul et al. [9] observed a 40% enhancement in the compressive strength of RuC when 20 wt.% of cement was replaced with equal amount of silica fume and fly ash. This enhancement was attributed to the better particle packing and cohesion of the concrete mix as a result of the reactivity of these materials and the consequent pozzolanic reaction.

The addition of fibres to RuC can enhance the mechanical performance of these composite concretes. Xie et al. [13] reported that the inclusion of manufactured steel fibres (MSF) in RuC, mitigated the reduction in compressive strength while increasing residual flexural strength. Similar outcomes were reported in other studies by the authors [1, 2] where SFRRuC presented better mechanical properties than plain RuC. Although the fresh and mechanical properties of RuC and SFRRuC have been studied by several researchers, there is still a dearth of data in this field, especially when rubber aggregates are incorporated in the large volumes (exceeding 20% replacement by volume of total natural aggregates). It should be noted that, large volumes of rubber aggregates replacements in concrete are necessary to attain flexibility in concrete pavements.

Few studies examined the durability and transport properties of RuC, with notable discrepancies being reported on the effect of rubber particles on long-term performance. Water permeability and water absorption by immersion generally increase with rubber content [14-16]. This has been attributed to the additional water required in RuC mixes to maintain workability, and the high void volumes between rubber particles and cement paste due to the hydrophobicity of rubber. Conversely, several researchers have observed a reduction in water absorption of RuC (up to 12.5% rubber for fine aggregates) using the method of immersion and related this behaviour to the impervious nature of rubber particles. Benazzouk et al. [17] reports that the addition of rubber crumbs of up to 40% volume in cement pastes reduced sorptivity, hydraulic diffusivity and air permeability. Similar observations are reported by Segre and Joekes [18] who also attributed this behaviour to the hydrophobic nature of rubber. The transport properties of these composite concretes are strongly dependent on the distinctive features of the starting concrete matrix, whose performance can significantly vary as a function of mix design, age and curing conditions, among other factors, which explains the variability in results obtained from different investigations.

In a recent study, the authors [1] studied the mechanical properties of SFRRuC mixes in which fine and coarse aggregates were partially replaced with rubber (0%, 20%, 40% or 60% replacement by volume), and different types of steel fibres (MSF and/or recycled tyre steel fibres- RTSF) added in volumes of up to 40 kg/ m^3. In addition to the increased toughness and flexibility attained, it was observed that all the examined SFRRuC mixes were able to achieve flexural strengths that meet the flexural strength limits prescribed in pavement design EN 13877-1 [19]. Concrete pavement slabs, however, are susceptible to several deteriorative processes that can be caused by the ingress of aggressive substances into concrete, such as corrosion due to attack by chlorides or carbonation. The rate of transport of aggressive agents is related to a large degree to the concrete's degree of saturation and air permeability [17]. Aggressive substances such as chlorides can also penetrate into concrete due to diffusion and capillary action.

The chloride permeability in RuC remains largely unknown and studies examining this [20, 21] reveal increased chloride permeability with rubber content, which can be significantly reduced with the addition of fly ash and/or silicate fume. This is consistent with the reduced water absorption and permeability achieved in concretes with these additions [15, 20]. To date, there are very few studies on the transport and durability properties of RuC with large volumes of rubber replacement [7, 22, 23], while the transport and durability properties of SFRRuC has not been studied yet. Furthermore, there is limited understanding on the mechanism governing chloride-induced corrosion of steel fibres in RuC and its potential effect on long-term performance. However, there is a good consensus that the main factors controlling durability of SFRC, when exposed to chlorides, include: (i) the age and the exposure conditions, (ii) the steel fibre type and size, (iii) the concrete matrix quality and (iv) the presence of cracks [24]. Consequently, it is important to understand the transport and durability properties of SFRRuC before using it in flexible concrete pavements.

In this study, the fresh state, mechanical strength, and transport properties of SFRC, and SFRRuC are investigated and compared. The fresh properties assessed include workability, air content and fresh density. The mechanical performance is examined in terms of compressive strength and flexural behaviour including flexural strength, elastic modulus and residual flexural strength. The transport properties examined are volume of permeable voids, gas permeability, sorptivity and chloride penetrability (chloride ion penetration depth and diffusion). The chloride corrosion effects due to exposure to a simulated accelerated marine environment (intermittent wet-dry cycles in 3% NaCl solution) are also evaluated.

2 Experimental Programme

2.1 Materials and mix designs

2.1.1 Materials

A Portland limestone cement CEM II-52.5 N, in compliance with EN 197-1 [25] and containing 80-94% Portland cement clinker, 10 –15% limestone and 0-5% minor additional constituents, was adopted as the primary binder in this study. Silica fume (SF) and fuel ash (FA) were also used (10 wt.% for each) to improve particle packing (or filling) in the mixture [9] as well as to reduce permeability and enhance concrete strength. Two types of high range water reducer HRWR admixtures, plasticiser and superplasticiser, were also added to achieve the desired workability. A water/binder (Portland cements + silica fume + fly ash) ratio of 0.35 was used in all mixes.

The coarse aggregates were river gravel with particle sizes of 5/10 mm and 10/20 mm, specific gravity (SG) of 2.65 and water absorption (A) of 1.2%. The fine aggregates were river sand with particles sizes of 0/5 mm, SG of 2.64 and A of 0.5%.

The rubber aggregates were recovered by the mechanical shredding of vehicular tyres. Rubber particles were sourced in the following size ranges: 0/0.5 mm, 0.5/2 mm and 2/6 mm, 5/10 mm, and 10/20 mm. A relative density of 0.8 (measured using a representative volume of rubber) was used for the rubber to determine the appropriate replacement by volume. Fig. 1 shows the particles size distribution for the used natural (N) and rubber (R) aggregates, obtained according to ASTM C136 [26].

A blend of two different types of steel fibres were used: 1) undulated MSF, and b) cleaned and screened recycled tyre steel fibres (RTSF). The physical and mechanical properties of both types of steel fibre are shown in Table 1.

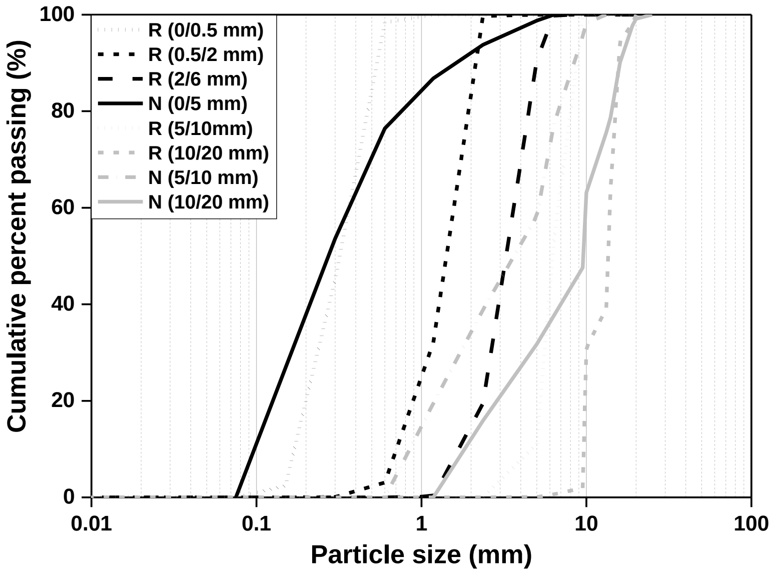

Fig. 1 Particle size distributions for natural aggregates and rubber particles

Table 1. Physical and mechanical properties of steel fibres

Fibre type	Length (mm)	Diameter (mm)	Density (g/cm3)	Tensile strength MPa
MSF	55	0.8	7.8	1100
RTSF	15-45 (> 60% by mass)	<0.3	7.8	2000

2.1.2 Concrete mix designs

An optimized conventional concrete mix design [9] with target cylinder compressive strength of 60 MPa at 28 days of curing, typically used in bridge piers for XD3 exposure class, was adopted in this study. It was confirmed by the authors in a previous study [1] that this mix design suites the replacement up to 60% of WTR and does not cause much degradation in concrete fresh properties, yet maintaining a mechanical performance suitable for pavement construction.

The key parameters examined experimentally are: (i) the content of rubber (0%, 30% and 60%) replacing both fine and coarse aggregates by volume, (ii) the content of fibres (0 or a blend of 20 kg/m^3 MSF + 20 kg/m^3 RTSF), (iii) the curing conditions (mist room or 3% NaCl), (iv) the age of testing (28, 90, 150 or 300 days).

Table 2 shows the rubber replacement ratios and fibre contents of the four mixes examined in this study. The mix nomenclature is described below: Each mix name follows the format NM, where N stands for the percentage of aggregate replacement (0 – conventional concrete with no rubber replacement, 30 or 60%), whilst M shows information about the reinforcement; P stands for plain concrete without fibres and BF stands for blended fibre mixes consisting 20 kg/m^3 of MSF and 20 kg/m^3 of RTSF). For example, 60BF mix contains 60% rubber replacement and contains both MSF (20 kg/m^3) and RTSF (20 kg/m^3). Table 3 presents the concrete mix designs per m^3 of concrete.

Table 2. Concrete mix ID and variables

Concrete mixes ID	% Rubber replacing aggregates by volume		MSF (kg/m^3)	RTSF (kg/m^3)
	Fine	Coarse		
0P	0	0	0	0
0BF	0	0	20	20
30BF	30	30	20	20
60BF	60	60	20	20

Table 3. Mixes proportions for 1 m^3 of fresh concrete

Components	Concrete mixes			
	0P	0BF	30BF	60BF
CEM II (kg/m^3)	340	340	340	340
SF (kg/m^3)	42.5	42.5	42.5	42.5
FA (kg/m^3)	42.5	42.5	42.5	42.5
Water (l/m3)	150	150	150	150
Plasticiser (l/m^3)	2.5	2.5	3.25	4.25
Superplasticiser (l/m^3)	5.1	5.1	5.1	5.1
Natural aggregates				
0/5 mm (kg/m^3)	820	820	574	328
5/10 mm (kg/m^3)	364	364	254	146
10/20 mm (kg/m^3)	637	637	446	255
Rubber				
0/0.5 mm (kg/m^3)	0	0	16.5	33
0.5/2 mm (kg/m^3)	0	0	24.8	49.6
2/6 mm (kg/m^3)	0	0	33	66
5/10 mm (kg/m^3)	0	0	33	66
10/20 mm (kg/m^3)	0	0	57.7	115.4
Fibres				
MSF (kg/m^3)	0	20	20	20
RTSF (kg/m^3)	0	20	20	20

2.1.3 Mixing, casting and curing procedure

Due to the limited capacity of the pan mixer used, each mix was cast in three batches. The concrete constituents were mixed according to the sequence shown in Fig. 2.

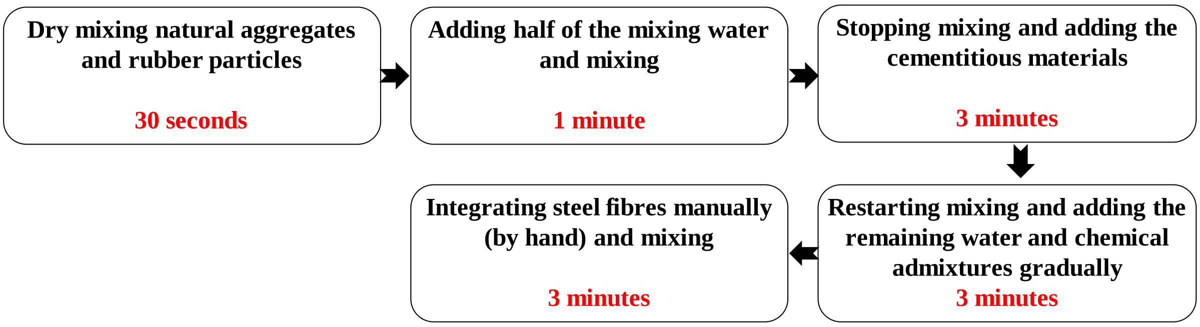

Fig. 2 Sequence of mixing

Concrete was cast in two layers (according to EN 12390-2) [27] and vibrated on a shaking table (25s per layer). The fresh concrete was covered with plastic sheets and left under standard laboratory conditions (20 $^{\circ}$C $\pm$ 2 and 50 $\pm$ 5% relative humidity (RH)) for 48 h. The specimens were then demoulded and stored in a mist room (21 $^{\circ}$C $\pm$ 2 and 95 $\pm$ 5% RH) to cure for 28 days. Following a period of 21 days, the 150 x 300 mm and 100 x 200 mm cylinders were removed from the mist room and sliced up, parallel to the trowelled surface, into five shorter cylinders (150 x 50 mm each) and two shorter cylinders (100 x 100 mm each), respectively. All concrete slices were placed back in the mist room until the end of mist curing (28 days).

2.2 Testing methods

2.2.1 Fresh state properties

Fresh concrete properties were assessed in terms of slump, air content and fresh density according to EN 12350-2 [28], EN 12350-7 [29], and EN 12350-6 [30], respectively.

2.2.2 Mechanical strength tests

Compression and flexural tests were performed on all of the specimens at the end of the drying period (4 days after removal from the mist room or NaCl solution). Three specimens were tested for each mix and environmental conditioning.

The Uniaxial compression tests were performed on concrete cubes (100 x 100 mm) according to EN 12390-3:2009 [31] at a loading rate of 0.4 MPa/s. Three-point bending tests were performed on prisms (100 x 100 x 500 mm) with 300 mm span, using an electromagnetic universal testing machine and a set-up similar to that suggested by RILEM [32]. A day before testing, a notch (5 mm thick and 15 mm deep) was sawn at the mid-span of the bottom side of each prism to force the crack to open at mid-span and a clip gauge was mounted across the notch (gauge length 5 mm) to measure the crack mouth opening displacement (CMOD) and control the test. All tests were CMOD-controlled at a constant rate of 0.05 mm/min for CMOD from 0 to 0.1 mm, 0.2 mm/min for CMOD ranging from 0.1 to 4 mm and 0.8 mm/min for CMOD from 4 mm to 8 mm. The net mid-span deflection was measured using two linear variable differential transformers (LVDTs) mounted at the middle of a yoke (one on each side), as suggested by JSCE [33].

2.2.3 Gas and water permeability

Cylinders of 150 x 50 mm were tested after 28 and 300 days of curing in a mist room. Prior to testing, specimens were pre-conditioned (oven dried) to remove water from the concrete pores. Rather than using the standardised preconditioning temperature of 105 ºC, which causes cracking, mainly due to the removal of interlayer and bound water present in the hydration products [34-36], a temperature of 80 ºC was initially used on the 28 day specimens in an attempt to minimise cracking. Constant mass was achieved after 7 days of drying, but SFRRuC specimens exhibited cracks of average width around 0.065 mm which can be attributed to the different coefficient of thermal expansion of the rubber aggregates. Although the values obtained from the cracked specimens are not expected to reflect the real permeability of SFRRuC, these values are still reported in the following and commented upon.

To minimise cracking induced during preconditioning, a reduced temperature of 40 ºC was adopted for treating the 300 day specimens. As expected, it took much longer to reach constant mass (between 30 to 40 days). Considering the extended time required to dry the concretes, it was decided not to expose the specimens to wet-dry chlorides exposure, as a direct correlation between gas and water permeability measurement and chloride penetrability would not be fair, as the concretes would have completely different ages by the time each of test was conducted.

Oxygen permeability tests were performed on three 150 x 50 mm cylinders per mix following the procedure recommended by RILEM TC 116-PCD-C [37], also called “Cembureau method”, using 1 Bar of oxygen gas above the atmospheric pressure. Sorptivity measurements were conducted in two cylinders of similar size following the recommendation of the EN 13057 [38]. After performing the sorptivity test, the same cylinders were used to measure the volume of permeable voids (VPV) based on the procedures of ASTM C1202 [39], also called the vacuum saturation method.

2.2.4 Chloride permeability and corrosion

After 28 days of mist curing, chloride permeability was evaluated in two different exposure conditions: (i) fully immersing cylinders (100 x 100 mm) in a 3% NaCl solution (placed in sealed plastic containers in the mist room until testing); and (ii) wet-dry cycles (accelerated chloride corrosion simulation), by immersion in a 3% NaCl for 4 days followed by a drying period in standard laboratory environmental conditions for 3 days. Prisms (100 x 100 x 500 mm), cubes (100 mm) and cylinders (100 x 100 mm) were kept apart by at least 10 mm using a specially designed frame. All specimens were preconditioned for ion chloride penetration tests using the unidirectional non-steady state chloride diffusion-immersion method described in EN 12390-11 [40].

After preconditioning for 90, 150 and 300 days in NaCl solution, two 100 x 100 mm cylinders per mix per condition were split into two halves at mid-point according to the colorimetric method [41, 42]. From each freshly split cylinder, the piece with the split section nearly perpendicular to the exposed surface was chosen for the penetration depth measurement, and was immediately sprayed with 0.1 N silver nitrate ($AgNO_3$) solution. Silver nitrate reacts with the chloride ion present in the hardened matrix to form white AgCl (white in colour); whereas at greater depth, silver nitrate reacts with the hydroxyl ion to form Ag_2O (dark brown), as described in formulas (1) and (2) [43].

$$Ag^{+} + \ Cl^{-} \rightarrow \ AgCl \downarrow (silver - white) \tag{1}$$

$$Ag^{+} + \ OH \ \rightarrow \ AgOH \ \rightarrow Ag_2O \downarrow (brown) \tag{2}$$

Chloride penetration depth was indicated by the boundary colour change within 10-15 minutes after spraying. The chloride penetration depth was marked at the colour change boundary and the depth was recorded as the average distance, taken from five sections (Fig. 3). The cylinder that registered the maximum average depth was selected for analysis and used to drill out binder powder from the surface and colour change boundary to determine acid-soluble chloride concentrations.

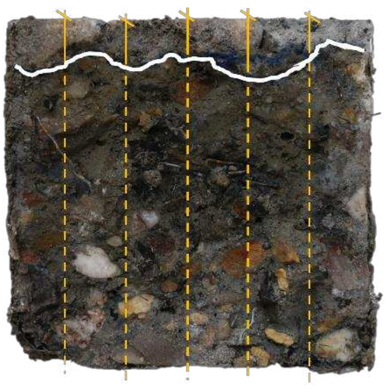

Fig. 3 Representative SFFRuC freshly split, sprayed and marked for determination of chloride penetration depth

The acid-soluble (total) chloride concentration was measured at the 134.724 emission line using a Spectro-Ciros-Vision ICP-OES instrument which was calibrated with standards of known chloride concentrations made up in 20% nitric acid. The apparent chloride diffusion coefficients (D_{app}) were roughly estimated using the re-arrange error function solution of Fick's second law of diffusion shown in Eq. (3) [41, 42]:

$$D_{app} = \left(\frac{x}{2 - erf^{-1}\left(1 - \frac{C_x}{C_s}\right)\sqrt{t}} \right) \tag{3}$$

where x is the maximum average distance of colour change boundary from the concrete surface; C_x is the total chloride concentration at the colour change boundary at any time t; C_s is the total chloride concentration at the surface.

It should be noted that the D_{app} obtained using the traditional profile method specified in EN 12390-11 [40] is more accurate than that of colorimetric method. This is due to the fact that the measurements and calculations of chloride concentration using colorimetric method can be influenced by many factors including concrete alkalinity, the amount and concentration of the sprayed $AgNO_3$ solution, pore solution volume of concrete, sampling method as well as method used for measuring the chloride content [42]. However, the colorimetric method is a quick, simple and relevant method for assessing the kinetics of chloride penetration in concrete specimens when non-steady state chloride diffusion test is carried out in laboratory condition. Many studies [41, 42, 44] have proven its feasibility to determine the average chloride penetration depth (the depth associated with the assumed ‘‘critical’’ chloride concentration with respect to corrosion risk ~ 0.4%. by unit mass of binder) and assess the D_{app}.

3 Results and Discussion

3.1 Fresh state properties

The slump, air content and fresh density of the concretes studied are presented in Table 4. The addition of fibres reduced the workability of the concrete, and this effect is more notable with the inclusion of both fibres and rubber in the SFRRuC mixes. For mixes 0BF, 30BF and 60BF, the slump drops by 5%, 13% and 56%, respectively, when compared with the plain concrete, 0P. The tendency of steel fibres to agglomerate contributed to the slump reduction. The decrease in slump as a result of adding rubber particles can be explained by the higher level of inter-particle friction between rubber particles and the other concrete constituents (owing to the rough surface texture and high coefficient of friction of rubber particles) [1, 4, 7-9]. Nevertheless, all mixes satisfy the slump requirements described in pavement design standard EN 13877-1 [19]. Moreover, similar to the finding in Ref. [9], no signs of segregation, bleeding or excessive “balling” were observed in any of the mixes.

Table 4. Fresh state properties of SFRRuC evaluated. Values in parenthesis correspond to one standard deviation of three measurements

Properties	Concrete mix			
	0P	0BF	30BF	60BF
Slump (mm)	223 (14)	212 (10)	193 (15)	98 (25)
Air content (%)	1.3 (0.5)	1.4 (0.1)	3.4 (1.1)	3.2 (0.2)
Fresh density (kg/m^3)	2405 (5)	2424 (9)	2124 (6)	1859 (4)

The addition of fibres alone did not induce notable changes in the air content of the concrete. The substitution of natural aggregate by rubber (mixes 30BF and 60 BF) in SFRC, however, significantly increased the air content of the fresh concrete by more than 100%. The rough and hydrophobic nature of rubber particles tends to repel water and therefore increases the amount of entrapped air in the mix. The increased friction between fibres and rubber also cause fibres to agglomerate and trap more air [1, 45].

The fresh density of the SFRC mix, 0BF, is slightly higher than that of the plain concrete mix, 0P, (Table 1) owing to the high specific gravity of the added fibres. The density of the fresh mix is significantly reduced when rubber particles are used to replace natural aggregates as a result of their lower density (Section 2.1.1). For the SFRRuC, 30BF and 60BF, the density decreases by 13% and 30%, respectively, compared to the plain concrete.

3.2 Effect of chloride exposure in mechanical performance

3.2.1 Visual inspection

Figs. 4 a) and b) show the appearance of specimens after 150 and 300 day exposure to accelerated chloride corrosion conditions, respectively. Prior to chloride exposure, there were no signs of rust on the concrete surface, which implies that the fibres were protected by a thin layer of cement paste. At the end of 150 days of wet-dry chloride exposure, however, the specimens showed minor signs of superficial rust (Fig. 4a) in regions where the fibres were near the concrete surface. A large amount of rust is observed on the surface of the specimens exposed for 300 days (Fig. 4b), mainly as a consequence of the corrosion of the steel frame used to hold the specimens. Nevertheless, at all periods of the accelerated chloride corrosion exposure, no sign of deterioration or cracks were observed on the concretes.

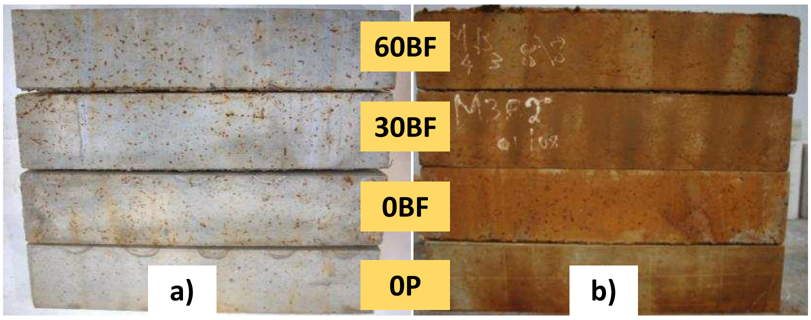

Fig. 4 SFRRuC specimens after a) 150 days, and b) 300 days of wet-dry chloride exposure

Fig. 5 shows the internal appearance of a SFRRuC splitted cube, 30BF, after 300 days of wet-dry chloride exposure. Despite the external rusty appearance (Fig. 4b), no evidence of rust is observed on the fibres embedded in these concretes. This indicates that steel reinforcement did not corrode to any significant extent under the wet-dry chloride exposure. This performance may be explained by the reduced chloride permeability of the concretes, as it will be discussed in detail in the following sections, and the discrete nature of steel fibres embedded in the matrix, generating smaller potential differences along the steel surface and reduced cathode/anode ratios compared to conventional steel rebars [24].

Fig. 5 Section through a SFRRuC specimen after 300 days of wet-dry chloride exposure

In addition, the dense and uniform fibre-matrix interfacial transition zone (ITZ), composed mainly of rich segregated lime, acts as a high alkalinity barrier and protects fibres in the bulk SFRC against chloride and oxygen ingress [24].

3.3 Compressive strength

The influence of wet-dry chloride exposure on the compressive strength of SFRRuC is presented in Fig. 6. Error bars represent one standard deviation of three measurements. Comparable compressive strength values are seen for the plain concrete, 0P, and the SFRC, 0BF, before and after chloride exposure. As expected, the replacement of natural aggregates with rubber particles led to a substantial reduction in compressive strength. Prior to chloride exposure, reductions of up to 54% and 86% in compressive strength, respectively, with respect to 0BF. The loss in compressive strength is mainly due to the lower stiffness and higher Poisson ratio of rubber in comparison to that of natural aggregates. The weak adhesion between cement paste and rubber particles may also contribute to the strength degradation, as discussed by the authors in Ref. [1] and Khaloo et al. in Ref. [12].

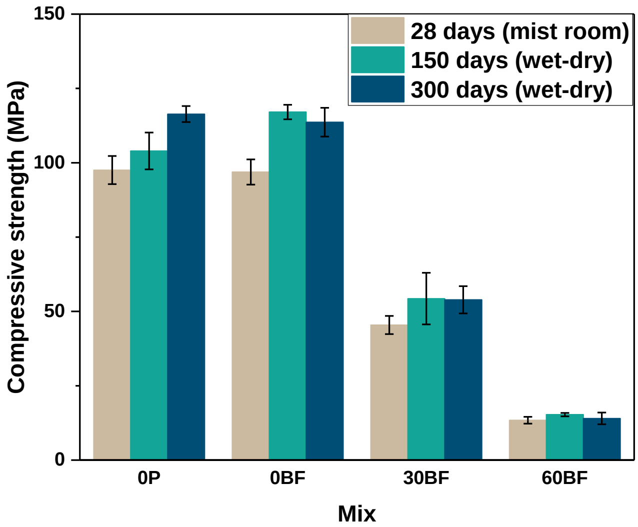

Fig. 6 Compressive strength of concretes assessed before and after 150 and 300 days of wet-dry chloride exposure

All mixes after 150 and 300 days of wet-dry chloride exposure present a slightly increased compressive strength, compared to the 28-day values measured prior to the chloride exposure. The increase in strength is attributed to the continuous hydration of the cementitious paste over the period of exposure, owing to the high amount of pozzolanic materials used for replacing Portland cement in all the concrete mixes.

3.4 Flexural behaviour

The mean values of flexural strength at 28 days and after150 and 300 days of wet-dry chloride exposure are presented in Fig. 7. Error bars represent one standard deviation of three measurements. The addition of fibres to plain concrete, mix 0BF, enhances the 28-day flexural strength by 28%, compared to 0P. The partial replacement of natural aggregates by rubber particles reduced the flexural strength of the tested concretes, but to a lesser extent than the compressive strength (Fig. 6). The 28-day flexural strength reduction of SFRRuC mixes, 30BF and 60BF, in comparison to 0BF is 31% and 56%, respectively. The contribution of steel fibres in enhancing the flexural strength was anticipated as the thin fibres, RTSF, tend to “sew” the micro-cracks that develop in the matrix during loading, while the thick fibres, MSF, tend to control the propagation of wider cracks and redistribute stresses [1, 46].

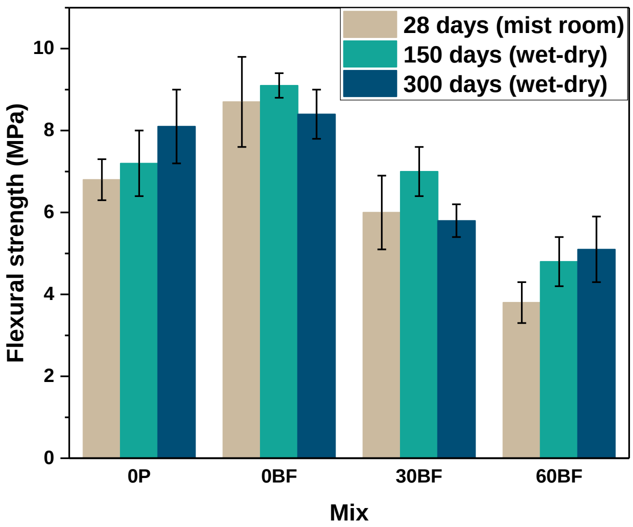

Fig. 7 Flexural strength of concretes assessed before and after 150 and 300 days of wet-dry chloride exposure

For all mixes, the flexural strength results are higher at the end of 150 days of wet-dry chloride exposure than those of 28-day mist cured specimens, as a consequence of the ongoing hydration of the cement in the concretes.

No clear trend can be identified in the flexural strength values of the specimens at the end of 300 days of wet-dry cycles. While 0P and 60BF mixes present higher flexural strength values, compared to those of 150 days of wet-dry cycles, the flexural strength values of 0BF and 30BF mixes are even lower than their respective strength at 28-days. This variation may be the result of the high natural variability in these specimens. It is unlikely that the flexural strength of 0BF and 30BF specimens was reduced due corrosion attack, as evidence of rust in the fibres embedded in these specimens was not observed (see Section 3.2.1).

Fig. 8 shows the average elastic modulus obtained from three prisms per mix over the three periods of testing. Error bars represent one standard deviation of three measurements. Flexural elastic modulus was determined based on the theory elastic deflection and by using the secant modulus of the load-deflection curves (from 0 to 30% of the peak load).

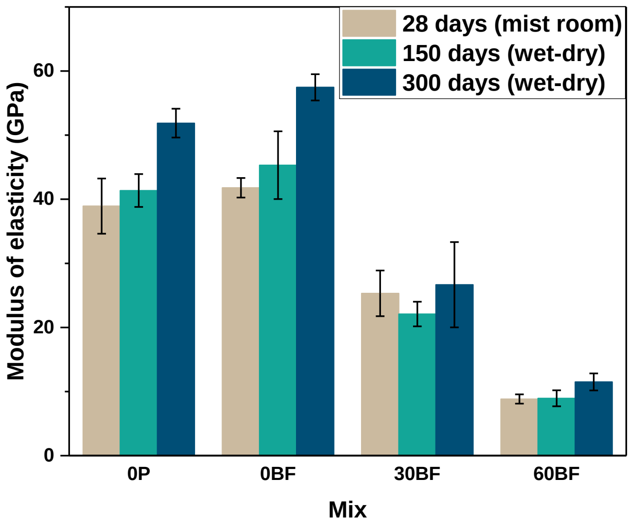

Fig. 8 Elastic modulus of all tested concrete specimens before and after 150 and 300 days of wet-dry chloride exposure

The addition of 40 kg/m^3 of fibres did not affect the elastic modulus of concrete by much. However, a notable decrease in the elastic modulus is observed from the replacement of natural aggregates with rubber particles; reductions up to 38% for 30BF and 79% for 60BF compared to 0BF. The reduction in the elastic modulus is mainly caused by the low stiffness of the rubber particles and to a lower degree by the high air content in these concretes, as discussed in section 3.1. The low elastic modulus of 60BF, however, is still comparable to that of typical of flexible pavements, i.e. around 8 GPa [47].

A general increase in the average elastic modulus of all mixes after 150 and 300 days of wet-dry cycles was identified, compared to 28-day compressive strength. Although enhancement in elastic modulus was expected as the compressive strength increases with time, the large increase seen for normal concrete after 300 days can be partly attributed to variability between the three prisms which came from three different batches, and partly to the fact that the elastic modulus is determined indirectly from deflections.

Fig. 9 presents the average flexural stress-CMOD curves registered in all prisms over the three periods of testing. The sudden stress loss after the peak load for the plain concrete mixes indicates their brittle behaviour in tension. On the other hand, all SFRC and SFRRuC mixes show enhanced post-cracking load bearing capacity and significant energy absorption. This is a result of the fibres bridging the cracks and controlling their propagation even after the peak load, dissipating energy through pull-out and mobilising and fracturing a larger volume of concrete. It is also evident that the post-peak energy absorption behaviour of the SFRC and SFRRuC specimens is not reduced after exposure to wet-dry cycles. This confirms that steel reinforcement did not corrode to any significant extent under the wet-dry chloride exposure adopted in this study.

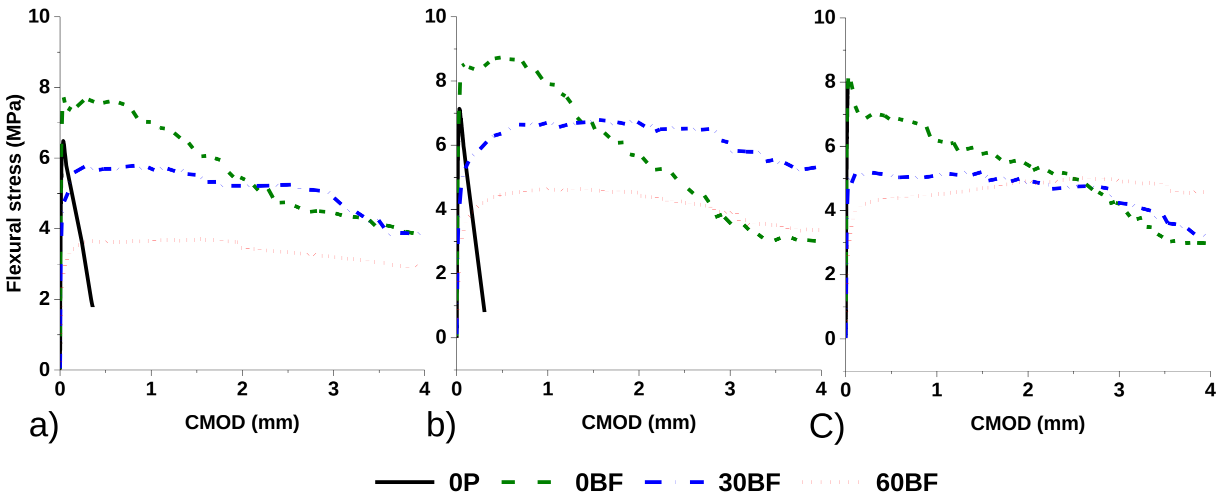

Fig. 9 Flexural stress-CMOD curves of the tested concrete specimens a) before, and after wet-dry chlorides exposure for b) 150 and c) 300 days

3.5 Transport properties

3.5.1 Evaporable moisture and volume of permeable voids

The loss of mass due to water evaporation after preconditioning the specimens at 80 ºC (28 day cured) and 40 ºC (300 day cured) was determined as the ratio between the total amount of evaporated water and the dry mass of the specimen. The mean values (average of five measurements) of evaporable moisture concentrations results, W_e, are shown in Fig. 10a, and the volume of permeable voids, VPV, are presented in Fig. 10b. Error bars correspond to one standard deviation of five measurements for W_e and two measurements for VPV. A direct relationship between the W_e and VPV is observed for all the tested concretes, independently of the preconditioning temperature and curing age, where higher values of evaporated water are obtained in more porous concretes.

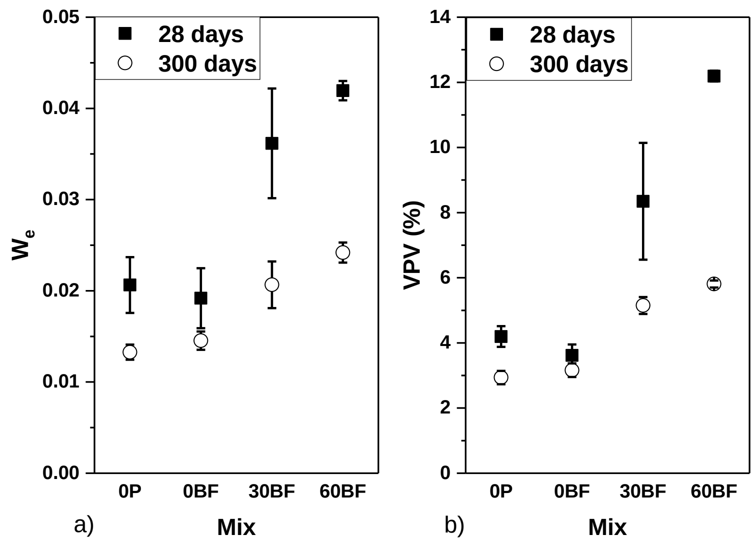

Figs. 10 a) Evaporable moisture, and b) volume of permeable voids of all tested concretes

The addition of fibres generally results in reduced shrinkage cracking and in the establishment of more tortuous and disconnected pore network [48], thus reducing VPV. For 28 days cured samples, 0BF mix exhibits, as expected, a decrease in VPV, though marginal and within the observed experimental error (average of 13%), whereas the SFRRuC mixes exhibit a large increase in VPV. This can be attributed to the rubber particles, the rough surface and hydrophobic nature of which can help trap air on their surface and make their interface more porous and highly absorptive to water [49, 50].

Minor changes in the VPV values are observed in concretes 0P and 0BF for the two curing conditions. This is unexpected as more mature concretes typically have lower permeability, but it may be the result of the already high quality of the concrete matrix which makes it dense to start with. In concrete composites with rubber aggregates, 30BF and 60BF, extended curing times reduce the VPV values by 24% and 93%, respectively. It should be pointed out that SFRRuC specimens exhibited severe cracking upon preconditioning at 80°C, which increased their permeability and caused the high VPV results recorded.

Baroghel-Bouny [51] proposed a classification of the durability of reinforced concrete structures based on "universal" durability indicators determined on a broad range of concretes cured in water. According to the proposed system, concrete mixes with VPV between 6-9% are categorised as highly durable. The VPV values of all the mixes examined in this study are lower than 6%, after 300 days of curing, even when rubber particles are used as partial aggregate replacement, which puts them in the highly durable category.

3.5.2 Oxygen permeability

The oxygen permeability is not only influenced by the overall porosity, but also by the proportion of continuity of larger pores where most of the flow will occur [52, 53]. Fig. 11 shows the oxygen permeability results for 28 day cured specimens (preconditioned at 80 ºC) and 300 day cured specimens (preconditioned at 40 ºC), expressed as the intrinsic permeability 'K'. Error bars correspond to one standard deviation of three measurements. Due to the extremely high permeability of the specimens resulting from the surface cracking upon preconditioning at 80°C, the gas permeability for the 28 day cured specimens with rubber particles could not be determined (the oxygen found its way out very quickly).

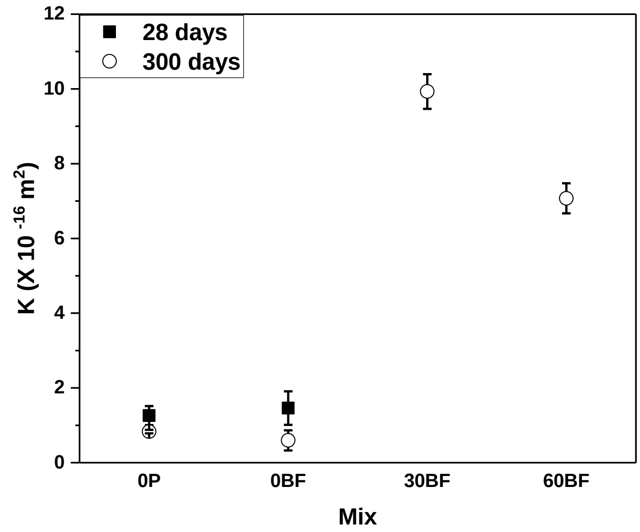

Fig. 11 Oxygen permeability results for all tested mixes

Considering the standard deviations as well as the experimental errors for both 28 and 300 days results, the oxygen permeability values for SFRC specimens, 0BF, are comparable with those of plain concrete, 0P, indicating that the fibres did not modify much the permeability of the concretes tested. SFRRuC specimens, 30BF and 60BF, on the other hand, show significantly higher permeability values, up to 12 and 8.5 times respectively, with respect to the plain concrete mix, 0P. These concretes presented comparable air contents (Table 4) and VPV values (Fig 10b), despite the differences in rubber content. The increased oxygen permeability recorded for the assessed specimens may be attributed to the compressibility of rubber particles when pressure is applied. As rubber deforms, the oxygen gas can more easily find its way through the specimen and around the rubber particles. If that is the case, then gas permeability may not be the best way to determine the permeability of RuC.

3.5.3 Water sorptivity

The main mechanism that governs sorptivity is capillary suction of water when a specimen is partially saturated [52, 54]. The difference in pressure causes the movement of water front through a porous material. Hence, sorptivity is derived by measuring the slope of the amount of water uptake per unit area as a function of the square root of time. The sorptivity results measured for 28 and 300 days cured specimens are shown in Fig. 12. Error bars correspond to one standard deviation of two measurements

For the 28 day cured samples, the addition of fibres to plain concrete, mix 0BF, causes marginal decrease in the sorptivity value, with an average of 12% with respect to the plain concrete mix, 0P. For 300 day, however, 0BF specimens record marginally higher sorptivity values, with an average of 9%, than that of 0P specimens. These results are in good agreement with the VPV values (Fig 10.b) confirming that the extended curing time had only a minor effect on the sorptivity and on the already high quality of the concrete matrix evaluated in this study.

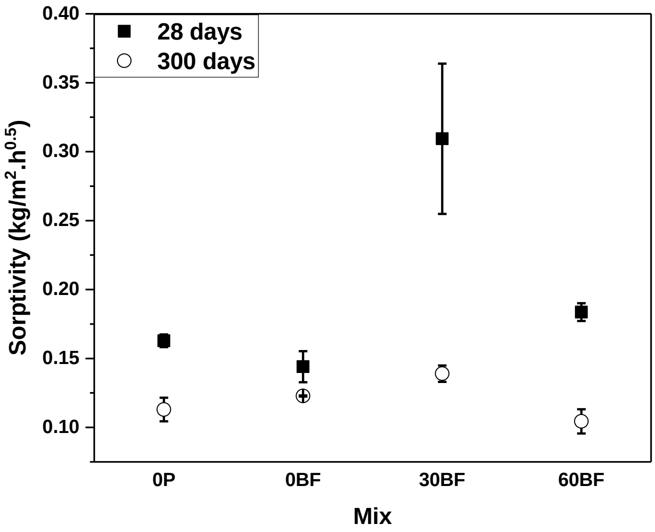

Fig. 12 Sorptivity values of all tested mixes

The 28 days sorptivity results of the SFRRuC specimens show different trends. While the 30BF specimens record the highest sorptiviy values, an average 90% higher than 0P mix, 60BF specimens shows slightly higher sorptivity value, average of 13% compared to 0P. Unlike VPV and chloride penetration tests, where the specimens are fully immersed for a long period of time, specimens evaluated for sorptivity were partially immersed in water (2 mm depth from the trowelled surface) and the water uptake measurements were recorded during the first 24 hours of first immersion, as specified in EN 13057 [38]. Therefore, the quality of the concrete surface that is in contact with water plays a major role in imbibing the water through the fine capillary pores. As it has been reported previously [45, 50], the rough texture of rubber particles cause both fine and coarse pores to increase with increasing rubber content. Hence, in addition to the surface cracking upon preconditioning at 80°C, the authors hypothesised that the high values of sorptivity for the 30BF specimens may be attributed to the large amount of fine pores which dominated the initial sorptivity behaviour. On the other hand, the high amount of large course rubber particles in the 60BF specimens located on the concrete surface in contact with water (see Fig. 13) could have limited the water absorption rate (owing to the non-sorptive nature of rubber particles) and dominated the initial sorptivity behaviour. To confirm this, the specimens were left partially immersed for a longer period (15 days) and the water uptake was measured. Similar to VPV, it was observed that the sorptivity of the concrete is higher with increasing the rubber content. This suggests that when water imbibed through the contact surface in 60BF, the amount of fine pores also dominated the water ingress into the sample consistent with the differences in pore network between the surface and the core of the specimens.

Fig. 13 Cross section view of the SFRRuC specimens used for the sorptivity test

Extending the curing time for 30BF and 60BF, i.e. 300 days, cause significant reduction in the sorptivity values, with average of 67% and 20%, respectively, when compared with the values registered for concretes cured for 28 days. This is mainly related to the absence of surface cracking upon preconditioning at 40°C which results in more realistic sorptivity values.

When calculating the concrete sorptivity using the depth penetration approach [52, 55, 56], all mixes examined here record sorptivity values less than 6 mm/h$^{0.5}$, which places them in the excellent durability class based on the durability index proposed by Alexander et al. [57] and adopted in Refs. [52, 55, 56].

3.6. Chloride ion penetration

Fig. 14 shows the chloride penetration zone after spraying 0.1 N $AgNO_3$ at the end of 90 and 150 days of chloride exposure in fully-saturated and wet-dry conditions. As the continuous hydration of concrete specimens that contain high amount of silica fume gradually darken the colour of the matrix (see Fig. 14), it was not possible to detect the penetration zone in any of the specimens exposed to chlorides for 300 days due to the similarity in colour between matrix and the rubber particles. This drawback of the colorimetric method for assessing chloride permeability in concretes containing blended cement and silica fume has also been previously reported [58].

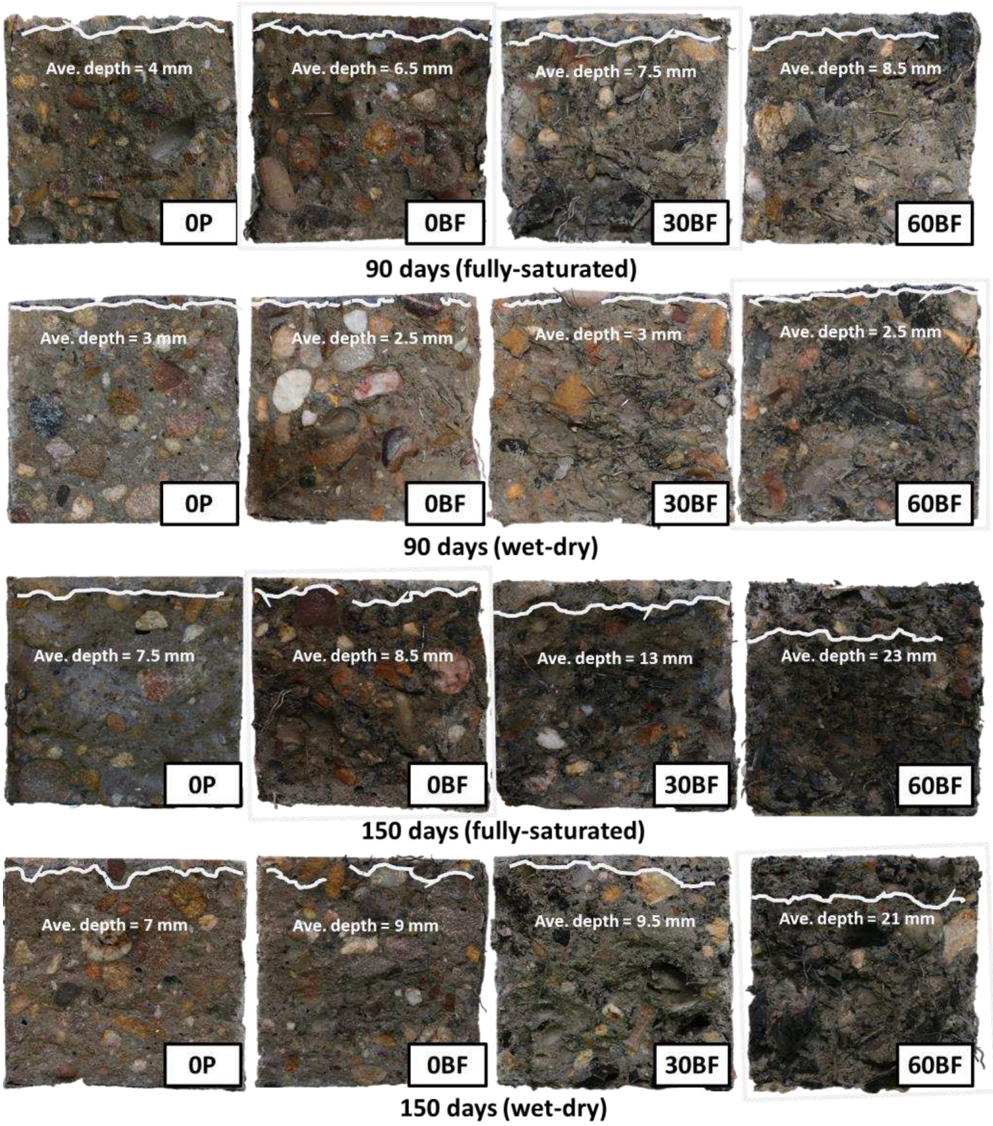

Fig. 14 Chloride contaminated zone of all concrete mixes at the end of 90 and 150 days of chloride exposure in fully-saturated and wet-dry conditions

Fig. 15 shows a comparison between the average chloride penetration depths for all concrete specimens. Error bars correspond to one standard deviation of the average depth measured in two different specimens. For concretes exposed to wet-dry cycles, the chloride penetration depth is in general lower than those of fully-saturated specimens. In fully-saturated specimens the chloride ingress is mainly governed by the diffusion mechanism. The process of chloride ingress into concrete exposed to wet-dry cycles is a combination of diffusion and absorption, as in partially saturated concretes the chloride solution is absorbed by capillary suction and concentrated by evaporation of water [59]. These results somehow contradict what has been reported for other blended cement concretes [59], where the wet-dry cycle exposure to chlorides typically leads to deeper chloride penetration compared to fully-saturated ones. The duration of the wet-dry cycles, and particularly the degree of dryness achieved, controls the extent of ingress of chlorides, as higher degrees of dryness facilitate deeper chloride penetration during subsequent wet cycles [60]. Due to the low permeability of these concretes, it seems the drying cycle was not sufficient to remove water beyond the concrete surface, hindering capillary sorption of chlorides rich solution into the concrete.

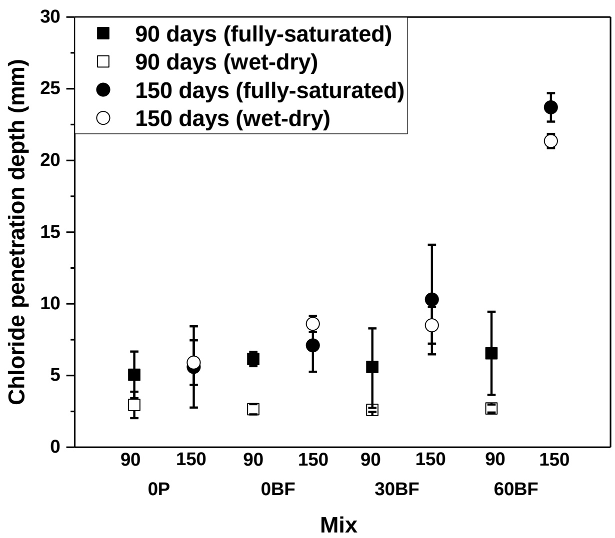

Fig. 15 Chloride penetration depth for all concrete mixes assessed at the end of 90 and 150 days of chloride exposure in fully-saturated and wet-dry conditions

The data presented in Fig. 15 also indicate that the chloride penetration depth at the end of 90 days of exposure was small and comparable, being in the range of 5–7 mm for the fully-saturated specimens, and 2–3 mm for the wet-dry specimens. This suggests that up to 90 days of chloride exposure, the penetration rate was not aggravated by the addition of rubber. At the end of 150 days of chloride exposure, however, the depth of chloride penetration in both conditions generally increased with rubber content. This is consistent with the higher values of VPV obtained for SFRRuC specimens (sections 3.5.1).

For practical purposes, due to the small chloride penetration depths at 90 days and difficulty in identifying chloride penetration depths at 300 days of chloride exposure, only specimens at 150 days of exposure (in both conditions) were considered for the determination of total chloride concentration and apparent chloride diffusion coefficient. Table 5 presents the total chloride concentrations by weight of binder as well as the roughly estimated apparent chloride diffusion coefficient measured at the colour change boundary for all of the assessed concretes. The chloride concentrations for the plain concrete and SFRC mixes, 0P and 0BF, were less than 10 ppm (i.e. the detection limit of the instrument used), hence it was not possible to detect the exact total chloride concentrations and then calculate the apparent diffusion coefficients for these mixes.

Table 5. Chloride concentration and the roughly estimated apparent chloride diffusion coefficient in concretes after 150 days of chlorides exposure

Mix	Maximum average chloride penetration depth, x (mm)		Chloride concentration at surface, C_s (wt% of binder)		Chloride concentration at colour change boundary, C_x (wt% of binder)		Apparent diffusion coefficient (10^{-12} m^2/s)	
	fully-saturated	wet-dry	fully-saturated	wet-dry	fully-saturated	wet-dry	fully-saturated	wet-dry
0P	7.6	7	0.159	0.640	<10 ppm	<10 ppm	-	-
0BF	8.58.	9	0.339	0.248	<10 ppm	<10 ppm	-	-
30BF	13	9.5	1.752	2.229	0.109	0.234	1.87	1.33
60BF	23	21	1.398	2.858	0.151	0.157	7.90	4.62

SFRRuC mixes, 30BF and 60BF, present lower chloride concentrations values (at both conditions) than 0.4% by weight of cement, which is the most commonly assumed critical total chloride concentration value inducing corrosion [58, 61]. This indicates that even with the increased VPV and sorptivity caused by the replacement of natural aggregates with rubber particles (Section 3.5.1 and 3.5.3), the assessed concretes present high resistance to chloride penetration for 150 days of chloride exposure.

SFRRuC mixes, 30BF and 60BF, show an increase in the apparent chloride diffusion coefficient at higher rubber contents, possibly due to their higher VPV and sorptivity. The apparent chloride diffusion coefficients of the fully-saturated and wet-dry specimens are comparable for the 30BF mixes, indicating that under the testing conditions used in this study, the drying cycle had a negligible effect on chloride penetration. Similar results have been identified in high quality Portland cement based concretes produced with silica fume, due to their refined porosity requiring longer drying times to obtain a particular moisture content [59]. Moreover, Kim et al. [44] evaluated the D_{app} at colour change boundary, following colorimetric method, for ordinary Portland concrete specimens made with 0.4 w/c ratio and immersed in marine environment for 6 months. It was found that the D_{app} was around 1.7 (10^{-12} m^2/s), in line with the values obtained here for 30BF. On the other hand, 60BF specimen in fully-saturated condition registers almost twice the diffusion coefficient than that in wet-dry condition. Nevertheless, with the apparent diffusion coefficients values observed here, SFRRuC mixes can be considered as medium to highly durable concrete mixes according to the durability indicators suggested in [51, 62].

For inspection purposes, the authors collected concrete samples at 50 mm depth from the exposed surface from those specimens exposed to chloride for 300 days, in both conditions, and the total chloride concentrations were measured. The total chloride concentrations for all of the examined samples were less than 10 ppm. This confirms the good resistance to chloride penetrability of all mixes.

4 Conclusion

This study examined the fresh, mechanical and transport properties as well as chloride corrosion effects in SFRRuC due to exposure to a simulated marine environment. Natural aggregates were partially replaced with waste tyre rubber particles and blends of MSF and RTSF were used as internal steel reinforcement. The following can be concluded:

- The addition of fibres marginally decreases workability and increases air content and unit weight. The substitution of rubber aggregates in SFRRuC mixes significantly reduces workability and unit weight (due to the lower density of rubber) and increases air content by more than 100%.

- No visual signs of deterioration or cracks (except superficial rust) were observed on the surface of concrete specimens subjected to 150 or 300 days of accelerated chloride exposure. Furthermore, no evidence of rust is observed internally on the fibres embedded in concretes indicating that steel reinforcement did not corrode to any significant extent under the wet-dry chloride exposure. This shows that blend fibres make a positive contribution to the durability of both conventional and RuC.

- The use of increasingly higher volumes of rubber aggregate in SFRRuC mixes reduces progressively the compressive strength and elastic modulus of concrete. Flexural strength is also affected, though to a lesser extent due to the presence of fibres. Hence, fibres are an essential component in the design of flexible concrete pavements.

- As a consequence of the ongoing hydration of the cementitious materials, a slight general increase in the mechanical properties of all mixes after 150 and 300 days of wet-dry chloride exposure was identified in comparison to the 28-day mechanical properties.

- While VPV and sorptivity generally increase with increased rubber content, the change with respect to plain concrete is minor. All mixes examined after 300 days of mist curing show VPV values lower than 6% and sorptivity values lower than 6 mm/h$^{0.5}$, which means that they can be classified as highly durable concrete mixes.

- The depth of chloride penetration in both conditions (fully-saturated and wet-dry) generally increases with rubber content. At the colour change boundary, 30BF and 60BF specimens record lower chloride concentrations than 0.4% by weight of cement (critical concentration inducing corrosion) and present apparent diffusion coefficients values within the range of highly durable concrete mixes.

It is concluded that the combination of rubber particles, up to 60%, and steel fibres can lead to an innovative concrete with increased ductility and flexibility as well as good transport characteristics. Future work should be focused on examining the capability of this promising concrete to withstand aggressive environments such as freeze-thaw resistance and fatigue performance.

Acknowledgements

The current experimental work was undertaken under the FP7 European funded collaborative project "Anagennisi: Innovative reuse of all tyre components in concrete" (Contract agreement number: 603722). The following companies offered materials and valuable in-kind contribution: Tarmac UK, Twincon Ltd, Aggregate Industries UK and Ltd Sika. Mr Alsaif would like to thank King Saud University and the Ministry of Education (Kingdom of Saudi Arabia) for sponsoring his PhD studies. Dr S.A. Bernal participation in this study has been sponsored by EPSRC through her ECF (EP/R001642/1).

References

1. Alsaif, A., et al., *Mechanical performance of steel fibre reinforced rubberised concrete for flexible concrete pavements.* Construction and Building Materials, 2018. **172**: p. 533-543.
2. Raffoul, S., et al., *Behaviour of unconfined and FRP-confined rubberised concrete in axial compression.* Construction and Building Materials, 2017. **147**: p. 388-397.
3. Hernández-Olivares, F. and G. Barluenga, *Fire performance of recycled rubber-filled high-strength concrete.* Cement and Concrete Research, 2004. **34**(1): p. 109-117.
4. Eldin, N.N. and A.B. Senouci, *Measurement and prediction of the strength of rubberized concrete.* Cement and Concrete Composites, 1994. **16**(4): p. 287-298.
5. Medina, N.F., et al., *Mechanical and thermal properties of concrete incorporating rubber and fibres from tyre recycling.* Construction and Building Materials, 2017. **144**: p. 563-573.
6. Flores-Medina, D., N.F. Medina, and F. Hernández-Olivares, *Static mechanical properties of waste rests of recycled rubber and high quality recycled rubber from crumbed tyres used as aggregate in dry consistency concretes.* Materials and Structures, 2014. **47**(7): p. 1185-1193.
7. Benazzouk, A., et al., *Physico-mechanical properties and water absorption of cement composite containing shredded rubber wastes.* Cement and Concrete Composites, 2007. **29**(10): p. 732-740.
8. Liu, F., et al., *Mechanical and fatigue performance of rubber concrete.* Construction and Building Materials, 2013. **47**: p. 711-719.
9. Raffoul, S., et al., *Optimisation of rubberised concrete with high rubber content: An experimental investigation.* Construction and Building Materials, 2016. **124**: p. 391-404.
10. Grinys, A., et al., *Fracture of concrete containing crumb rubber.* Journal of Civil Engineering and Management, 2013. **19**(3): p. 447-455.
11. Khatib, Z. and F. Bayomy, *Rubberized portland cement concrete.* Journal of Materials in Civil Engineering, 1999. **11**(3): p. 206-213.
12. Khaloo, A.R., M. Dehestani, and P. Rahmatabadi, *Mechanical properties of concrete containing a high volume of tire–rubber particles.* Waste Management, 2008. **28**(12): p. 2472-2482.
13. Xie, J.-H., et al., *Compressive and flexural behaviours of a new steel-fibre-reinforced recycled aggregate concrete with crumb rubber.* Construction and Building Materials, 2015. **79**: p. 263-272.
14. Turatsinze, A. and M. Garros, *On the modulus of elasticity and strain capacity of self-compacting concrete incorporating rubber aggregates.* Resources, conservation and recycling, 2008. **52**(10): p. 1209-1215.

15. Onuaguluchi, O. and D.K. Panesar, *Hardened properties of concrete mixtures containing pre-coated crumb rubber and silica fume.* Journal Of Cleaner Production, 2014. **82**: p. 125-131.
16. Bravo, M. and J. de Brito, *Concrete made with used tyre aggregate: durability-related performance.* Journal of Cleaner Production, 2012. **25**: p. 42-50.
17. Benazzouk, A., O. Douzane, and M. Quéneudec, *Transport of fluids in cement–rubber composites.* Cement and Concrete Composites, 2004. **26**(1): p. 21-29.
18. Segre, N. and I. Joekes, *Use of tire rubber particles as addition to cement paste.* Cement And Concrete Research, 2000. **30**(9): p. 1421-1425.
19. BSI, *EN 13877-1. Concrete pavements Part 1: Materials. BSI 389 Chiswick High Road London W4 4AL UK.* 2013.
20. Gesoğlu, M. and E. Güneyisi, *Permeability properties of self-compacting rubberized concretes.* Construction and Building Materials, 2011. **25**(8): p. 3319-3326.
21. Gesoglu, M. and E. Guneyisi, *Strength development and chloride penetration in rubberized concretes with and without silica fume.* Materials and Structures, 2007. **40**(9): p. 953-964.
22. Kardos, A.J. and S.A. Durham, *Strength, durability, and environmental properties of concrete utilizing recycled tire particles for pavement applications.* Construction and Building Materials, 2015. **98**: p. 832-845.
23. Topçu, İ.B. and A. Demir, *Durability of rubberized mortar and concrete.* Journal of Materials In Civil Engineering, 2007. **19**(2): p. 173-178.
24. Marcos-Meson, V., et al., *Corrosion resistance of steel fibre reinforced concrete - A literature review.* Cement and Concrete Research, 2018. **103**: p. 1-20.
25. BSI, *EN 197-1: Cement — Part 1: Composition, specifications and conformity criteria for common cements. BSI 389 Chiswick High Road, London W4 4AL, UK.* 2011.
26. ASTM, *C136: Standard test method for sieve analysis of fine and coarse aggregates. ASTM International, West Conshohocken, PA. doi:10.1520/C0136-06.* 2006.
27. BSI, *EN 12390-2: Testing hardened concrete, Part 2: Making and curing specimens for strength tests. BSI 389 Chiswick High Road, London W4 4AL, UK.* 2009.
28. BSI, *EN 12350-2: Testing fresh concrete, Part 2: Slump-test. BSI 389 Chiswick High Road, London W4 4AL, UK.* 2009.
29. BSI, *EN 12350-7: Testing fresh concrete, Part 7: Air content — Pressure. BSI 389 Chiswick High Road, London, W4 4AL, UK.* 2009.
30. BSI, *EN 12350-6: Testing fresh concrete Part 6: Density. BSI 389 Chiswick High Road, London, W4 4AL, UK.* 2009.
31. BSI, *EN 12390-3: Testing hardened concrete, Part3: Compressive strength of test specimens. BSI 389 Chiswick High Road, London W4 4AL, UK.* 2009.
32. RILEM, *TC 162-TDF: Test and design methods for steel fibre reinforced concrete, Bending test, Final Reccomendation. Materials and Structures: 35, 579-582.* 2002.
33. JSCE, *SF-4: Method of test for flexural strength and flexural toughness of steel fiber reinforced concrete. Japan Concrete Institute, Tokio, Japan.* 1984.
34. Feldman, R.F. and V.S. Ramachandran, *Differentiation of interlayer and adsorbed water in hydrated Portland cement by thermal analysis.* Cement And Concrete Research, 1971. **1**(6): p. 607-620.
35. Farage, M., J. Sercombe, and C. Galle, *Rehydration and microstructure of cement paste after heating at temperatures up to 300 C.* Cement And Concrete Research, 2003. **33**(7): p. 1047-1056.
36. Graeff, A., *Long Term Performance of Recycled Steel Fibre Reinforced Concrete for Pavement Applications*, in *Department of Civil and Structural Engineering*. 2011, The University of Sheffield: Sheffield.
37. RILEM, *TC 116-PCD: Test for gas permeability of concrete. A, B and C: Permeability of concrete as a criterion of its durability. Materials and Structures, 32, 174-179.* 1999.

38. BSI, *EN 13057:2002: Products and systems for the protection and repair of concrete structures - Test methods - Determination of resistance of capillary absorption. BSI 389 Chiswick High Road, London W4 4AL, UK.* 2002.
39. ASTM, C., *1202.* Rapid Chloride Permeability, 1997.
40. BSI, *EN 12390-11: Testing hardened concrete - Part 11: Determination of the chloride resistance of concrete, unidirectional diffusion. BSI 389 Chiswick High Road, London W4 4AL, UK.* 2015.
41. Baroghel-Bouny, V., et al., *AgNO3 spray tests: advantages, weaknesses, and various applications to quantify chloride ingress into concrete. Part 1: Non-steady-state diffusion tests and exposure to natural conditions.* Materials and structures, 2007. **40**(8): p. 759.
42. He, F., et al., *AgNO 3-based colorimetric methods for measurement of chloride penetration in concrete.* Construction and Building Materials, 2012. **26**(1): p. 1-8.
43. Ismail, I., et al., *Influence of fly ash on the water and chloride permeability of alkali-activated slag mortars and concretes.* Construction and Building Materials, 2013. **48**: p. 1187-1201.
44. Kim, M.-Y., E.-I. Yang, and S.-T. Yi, *Application of the colorimetric method to chloride diffusion evaluation in concrete structures.* Construction and Building Materials, 2013. **41**: p. 239-245.
45. Siddique, R. and T.R. Naik, *Properties of concrete containing scrap-tire rubber–an overview.* Waste Management, 2004. **24**(6): p. 563-569.
46. Hu, H., et al., *Mechanical properties of SFRC using blended manufactured and recycled tyre steel fibres.* Construction and Building Materials, 2018. **163**: p. 376-389.
47. Council of the European Union, *Council Directive 1999/31/EC of 26 April 1999 on the landfill of waste*. 1999.
48. Singh, A.P. and D. Singhal, *Permeability of steel fibre reinforced concrete influence of fibre parameters.* Procedia Engineering, 2011. **14**: p. 2823-2829.
49. Karahan, O., et al., *Fresh, Mechanical, Transport, and Durability Properties of Self-Consolidating Rubberized Concrete.* Aci Materials Journal, 2012. **109**(4).
50. Sukontasukkul, P. and K. Tiamlom, *Expansion under water and drying shrinkage of rubberized concrete mixed with crumb rubber with different size.* Construction And Building Materials, 2012. **29**: p. 520-526.
51. Baroghel-Bouny, V. *Evaluation and prediction of reinforced concrete durability by means of durability indicators. Part I: new performance-based approach*. in *ConcreteLife'06-International RILEM-JCI Seminar on Concrete Durability and Service Life Planning: Curing, Crack Control, Performance in Harsh Environments*. 2006: RILEM Publications SARL.
52. Du Preez, A. and M. Alexander, *A site study of durability indexes for concrete in marine conditions.* Materials and structures, 2004. **37**(3): p. 146-154.
53. Mackechnie, J.R., *Predictions of reinforced concrete durability in the marine environment*. 1995, University of Cape Town.
54. Pelisser, F., et al., *Concrete made with recycled tire rubber: effect of alkaline activation and silica fume addition.* Journal Of Cleaner Production, 2011. **19**(6): p. 757-763.
55. Olorunsogo, F. and N. Padayachee, *Performance of recycled aggregate concrete monitored by durability indexes.* Cement And Concrete Research, 2002. **32**(2): p. 179-185.
56. Alexander, M. and B. Magee, *Durability performance of concrete containing condensed silica fume.* Cement And Concrete Research, 1999. **29**(6): p. 917-922.
57. Alexander, M., J. Mackechnie, and Y. Ballim, *Guide to the use of durability indexes for achieving durability in concrete structures.* Research monograph, 1999. **2**.
58. Baroghel-Bouny, V., et al., *$AgNO_3$ spray tests: advantages, weaknesses, and various applications to quantify chloride ingress into concrete. Part 1: Non-steady-state diffusion tests and exposure to natural conditions.* Materials and Structures, 2007. **40**(8): p. 759-781.
59. Hong, K. and R.D. Hooton, *Effects of cyclic chloride exposure on penetration of concrete cover.* Cement and Concrete Research, 1999. **29**(9): p. 1379-1386.
60. Neville, A.M., *Properties of Concrete, 4th Ed.* 1996, Harlow, UK: John Wiley & Sons. 844.

61. Glass, G. and N. Buenfeld, *The presentation of the chloride threshold level for corrosion of steel in concrete.* Corrosion science, 1997. **39**(5): p. 1001-1013.

62. Assié, S., G. Escadeillas, and V. Waller, *Estimates of self-compacting concrete 'potential'durability.* Construction and Building Materials, 2007. **21**(10): p. 1909-1917.